Synthesis and characterization of amino-capped oligothiophene-based hole-transport materials†

Olivier Clot,[a] Don Selmarten*[a] and Michael J. McNevin[b]

Received 29th July 2005, Accepted 5th September 2005
First published as an Advance Article on the web 11th October 2005
DOI: 10.1039/b510826h

A series of seven thiophene-based oligomers were prepared as hole transport materials. The **DBAT*n*** series is composed of six oligothiophenes (n = 1–6) capped with two dibutylaminostyryl electron donating moieties. The band gaps for these compounds range from 2.47 to 2.19 eV. It was found that the bis(amino) substituents control the ionization potential, while the electron affinity and energy gap depend directly on the oligothiophene chain length. The bulk crystalline properties of these materials depend strongly on whether the number of thiophene rings in the bridge is even or odd. This results in the compounds that have an odd number of thiophene units in the bridge to exhibit depressed melting points with respect to the structures with an even number of rings. X-Ray structure determination was obtained from single crystals of **DBAT1** and **-2**. Good solubility, thermal stability and film forming properties were found throughout the series of compounds. A seventh compound, **DH2E4T**, was also prepared. This molecule is comparable to α,ω-dihexylsexithiophene but with greater solubility and reduced optical band gap (2.32 eV).

Introduction

In both the academic and industrial research community, an intense effort into the investigation of organic solar cells has recently emerged. Within the field of organic solar energy conversion there are several approaches that have been taken to achieve usable electricity from solar photons. Amongst these, we are investigating a variant of the dye sensitized "Grätzel" type cell.[1,2] The problem with these existing cells is that the hole conduction phase is a volatile organic electrolyte. Such a cell would not be practical when exposed to real-world outdoor conditions. In order for a solar cell that could function as a marketable product to be realized, a non-volatile hole transport medium is needed. For this reason we turned our attention to solid-state hole-conductive, pi-conjugated systems.

Pi-conjugated polymers are known to behave as hole conductors. For them to function well in a solar cell application, it would be a great benefit to understand their fundamental properties (electronic structure, physical ordering, *etc.*).[3] Attempting to interrogate the basic science of polymers can be challenging for several reasons. Therefore, we chose to focus our efforts on a series of tailored molecular moieties that are analogs to the conductive polymer poly(thiophene). Conjugated oligomers with well-defined chemical structures have received considerable attention as active materials in field-effect transistors, light emitting diodes, solar cells or electrographic materials.[4,5] Monodisperse oligomers allow for a precise control of the structure and relevant electronic properties such as ionization potential, electron affinity and energy gap. In this work, we have designed and prepared a series of thiophene-based π-conjugated compounds to be used as the solid-state hole transport layer (HTL) in sensitized solar cells (SSC).[2,6] The performance of solid-state SSCs partially depends on a rapid charge separation at the interface between the inorganic nanoporous electrode and the organic HTL. Therefore, a good energetic alignment between inorganic and organic semiconductors is of paramount importance. Another property that is important for cell performance is how well the polymer physically covers the metal oxide and fills the pores. Finally, even assuming perfect surface coverage and pore filling, said material must exhibit swift hole transport. Unlike the bulk heterojunction cell, which is concerned with exciton mobilities, we are interested in hole mobilities. Although very large hole mobilities have been reported for oligomers such as α,ω-dihexylsexithiophene (**DH6T**), the low solubility of that material has restricted device processing to vacuum deposition.[7,8] Not only is this process costly, such a technique is unlikely to completely fill the convoluted mesoporous structure of a SSC electrode. Therefore, along with efficient hole transport capability, we have pursued two main goals in the design of the oligomers: solubility and thermal stability. Improving on the solubility gives us the ability to solution process the HTL. Thermal stability allows for thermal annealing. This allows us to melt and or anneal the organic HTL and study the impact this has on the films properties. We have then chosen to design the **DBAT*n*** and **DH2E4T** oligomers (Chart 1) to mimic existing highly efficient hole transport compounds such as **DH6T** or **TPD**, but with improved solubility.

[a]*National Renewable Energy Laboratory, 1617 Cole Blvd, Golden, CO, 80401, USA. E-mail: don_selmarten@nrel.gov*
[b]*Department of Chemistry and Biochemistry, University of Colorado, Boulder, CO, USA 80309-0215*

† Electronic supplementary information (ESI) available: table of crystallographic data and collection parameters and complete tables of bond lengths and angles for **DBAT1** and **-2**. See DOI: 10.1039/b510826h

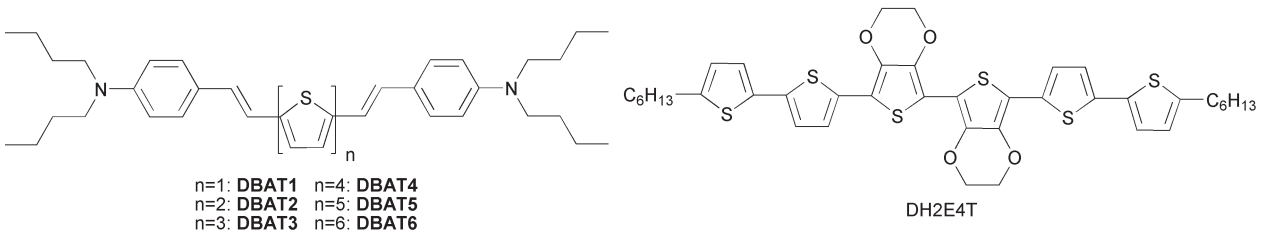

Chart 1 Compounds' structures

Results and discussion

Synthesis

DBAT1, **-2** and **-3** were prepared in 80, 74 and 76% yield respectively *via* a two-fold Horner–Emmons–Wittig olefination of the appropriate oligothiophene dialdehyde with dibutylaminobenzylphosphonate (Scheme 1a). Because of the poor solubility of oligothiophene dialdehydes beyond quaterthiophene, a Stille coupling in DMF was chosen as the route to prepare **DBAT4**, **-5** and **-6**. **DBAT4** was prepared by coupling **2** with dibromobithiophene with a 52% yield, while **DBAT5** and **-6** were prepared in 52 and 35% yield by coupling **3** with bis(tributylstannyl)thiophene or -bithiophene, respectively (Scheme 1a). The Horner–Emmons–Wittig olefination chosen to prepare **DBAT1**, **-2** and **-3** as well as the building blocks **2** and **3** favors the formation of E-isomers. It was confirmed by ^{1}H-NMR spectroscopy that, throughout the **DBAT*n*** series, all the compounds are pure E-isomers with a trans coupling constant of 16.0 Hz for the olefinic protons and that the compounds possess a center of symmetry as both olefin bonds are identical. All the compounds of the **DBAT*n*** series, except for **DBAT6**, have good solubilities (10 to 20 g L^{-1}) in common polar solvents such as methylene chloride, chloroform or THF. The solubility of **DBAT6** in the same solvents is lower (2–3 g L^{-1}) but remains significantly larger than that of **DH6T** (1 g L^{-1} in $CHCl_3$).[7] Such solubilities allow processing by spin-coating to form micron-thick films which is not possible with compounds such as **DH6T**. Compound **DH2E4T** was synthesized *via* Stille coupling between bis(stannyl)bis(EDOT) and bromohexylbithiophene and was obtained as an orange–red powder (Scheme 1b). Its solubility in chloroform was close to 2.5 g L^{-1}, which is 2.5 times that of the **DH6T** parent compound.[7]

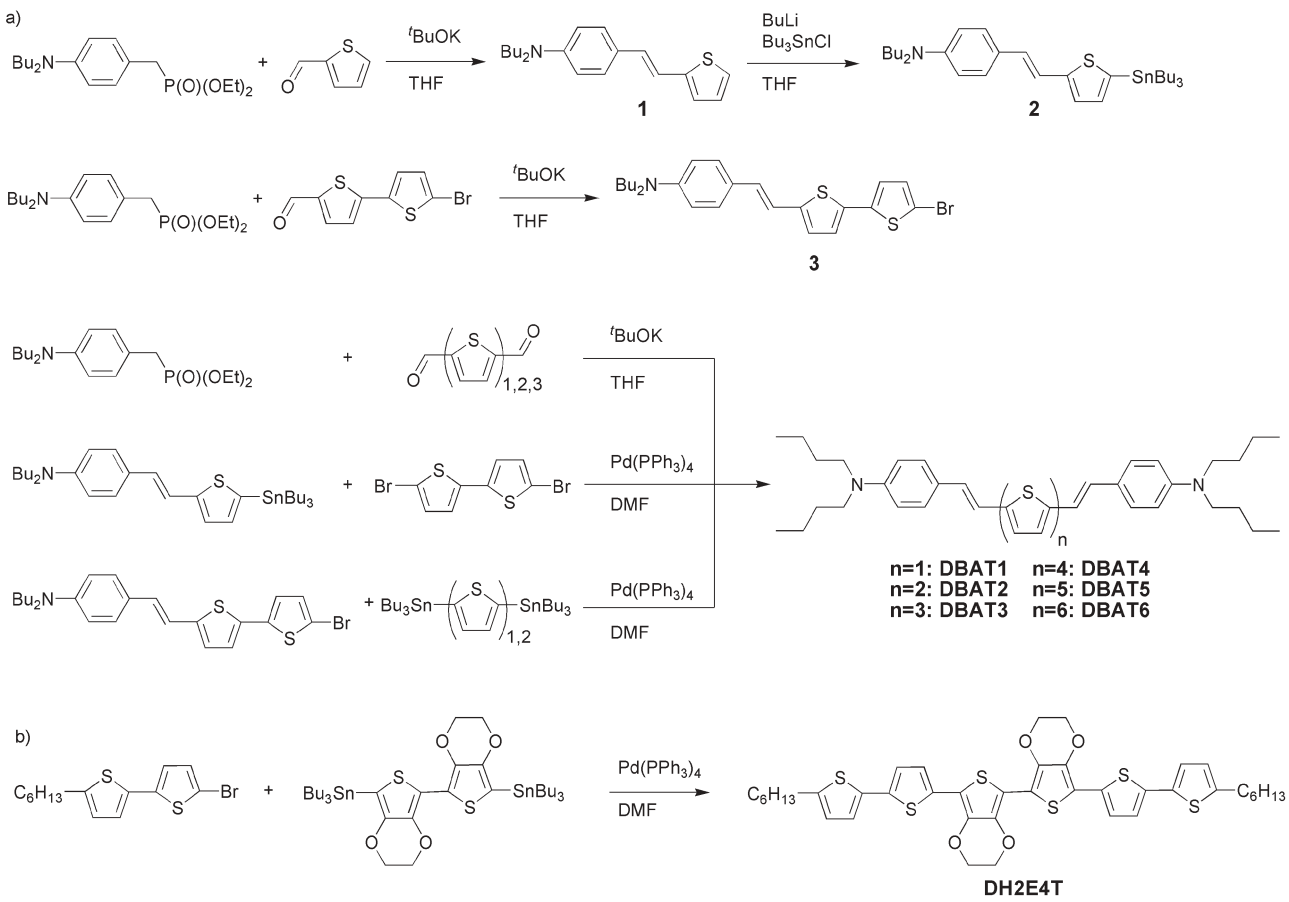

Scheme 1 Synthesis of the compounds.

Table 1 Thermal properties, UV-vis and fluorescence maxima

Compound	T_m[a]/°C	T_c[a]/°C	T_d/°C	λ_{max}[c]/nm (ε/L mol^{-1} cm^{-1})	E_g^{opt}[d]/eV	λ_{em}[ce]/nm
DBAT1	80–81	N/a	321	446 (4.64 × 10^4)	2.47	514
DBAT2	153–154	135–136	365	467 (4.95 × 10^4)	2.33	543
DBAT3	123–124	102–103	375	473 (4.74 × 10^4)	2.26	561
DBAT4	226–228	215–216	383	479 (5.99 × 10^4)	2.23	570
DBAT5	206–207	N/a	383	480 (5.78 × 10^4)	2.21	578
DBAT6	103–105[f] 274–276[g]	96–97[h]	390	489 (4.66 × 10^4)	2.19	580
DH2E4T	202–203	170–171	374	470 (6.17 × 10^4)	2.32	536, 571

[a] Measured by DSC, T_m (melting point at 10 °C min^{-1}) and T_c (crystallization point at 2 °C min^{-1}). [b] T_d (decomposition onset) measured by TGA (5 °C min^{-1}) in N_2. [c] In chloroform. [d] Calculated by extrapolation of the low-energy edge of the UV-vis absorption. [e] Excitation at λ_{max}. [f] Crystalline to amorphous glass transition. [g] Not present during the 2nd heating cycle. [h] Glass state crystallization.

Thermal behavior

The melting points of the compounds in the **DBAT*n*** series shown in Table 1 range between 80 (**DBAT1**) and 274 °C (**DBAT6**) while **DH2E4T** melts at 202 °C. An interesting trend was seen with the melting temperatures within the **DBAT*n*** series. Instead of monotonously increasing with the oligothiophene length, as it is generally the case for conjugated oligomers,[9,10] the melting points (MP) can be placed on two separate parallel lines (Fig. 1). The higher line contains the three compounds with an even number of thiophene units. While the lower line contains the remaining three compounds with an odd number of thiophene units. The melting temperatures did not depend on the solvent system used to recrystallize the compounds, although several different combinations were attempted for each structure. The same trend was observed within the series when considering the crystallization temperatures (T_c).

Although, with most unsubstituted or α,ω-substituted oligothiophenes, MPs are reported to monotonously increase with the chain length,[7,8,11,12] it also has been reported, for instance, within amine-[13] or α,ω-diformyl-substituted[14] oligothiophene series that the MP for the odd-numbered members are depressed. In the case of the **DBAT*n*** series, the MP trend is very clearly marked and is likely due to the symmetry of the structures that directs the crystal packing. This is supported by X-ray crystal structures and solid-state

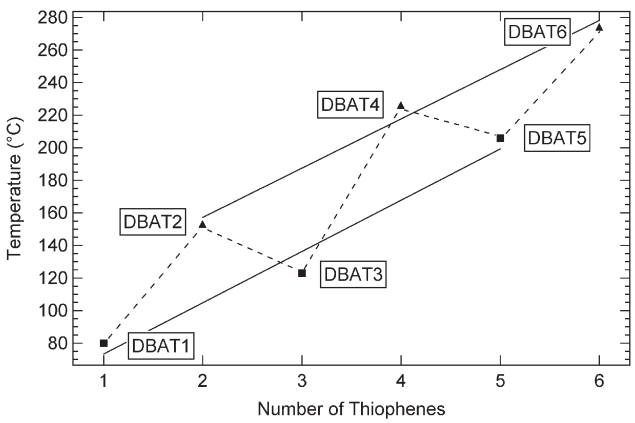

Fig. 1 Evolution of the melting temperature for the **DBAT*n*** series as a function of the odd (squares) and even (triangles) number of thiophene rings in the bridge. The lines are shown on the graph only to guide the eye.

^{13}C-NMR studies on various odd- and even-numbered oligothiophenes, which demonstrate the influence of the presence of a center of symmetry in the crystal packing and conformation of oligothiophenes.[15–17] This supposition is part confirmed by direct observation of the various compounds of the **DBAT*n*** series. While spin-coated films of **DBAT2** and **-4** are visually grainy and highly crystalline, **DBAT1**, **-3** and **-5** yield, under similar spin-coating conditions, very smooth and glassy films. Moreover, the DSC traces of **DBAT2**, **-4** and **-6** showed a very sharp and distinct endothermic transition at the melting point. In contrast, the transition recorded for **DBAT3** was broader and that of **DBAT5** almost indistinct. This indicates that in the solid-state, the **DBAT3** is less crystalline than **-2** or **-4** while **DBAT5** is almost amorphous. XRD studies on solid-state films as well as single crystal X-ray spectroscopy are under way in order to explain this interesting solid-state behavior.

The DSC trace for **DBAT6** displayed two endothermic peaks at 103 and 274 °C. The first peak was attributed to a solid-state transition to a glass state while the second was assigned to a solid–liquid transition. Upon cooling, only one exothermic transition was observed at 96 °C, and was attributed to the crystallization from an amorphous solid glass. After the first melt–cool cycle, the second heating only showed the lower endothermic transition at 104 °C. Even when heated up to 350 °C, the second melting endotherm was not seen. The second cooling cycle was identical to the first with only one transition at 96 °C.

Compound **DH2E4T** displayed a larger recrystallization point interval of 32 °C, which showed that the compound remained in a super-cooled liquid phase between 202 and 170 °C.

For all the compounds, T_d under nitrogen is significantly higher than their respective T_m under nitrogen (Table 1). Therefore, all compounds shown here satisfy the chemical stability requirements for thermal annealing. They can be heated into a liquid melt under nitrogen or vacuum in order to efficiently fill the pores of the inorganic SSC electrode without decomposition.

Crystal structures

Single crystals of **DBAT1** and **-2** were obtained from a chloroform–methanol mixture.‡ The X-ray structure determinations

‡ CCDC reference numbers 279764–279764. For crystallographic data in CIF format see DOI: 10.1039/b510826h

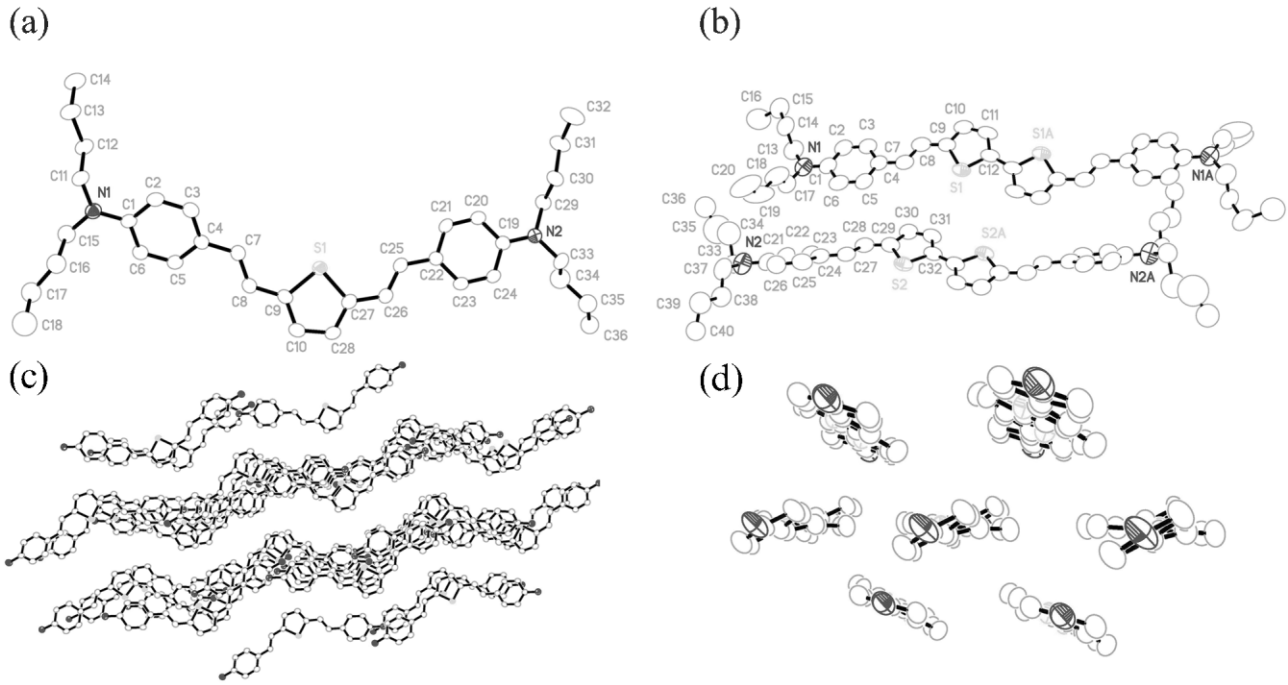

Fig. 2 (a) View of **DBAT1** structure, (b) view of **DBAT2** structure, (c) packing for **DBAT1**, the butyl chains were omitted for clarity and (d) herringbone packing for **DBAT2**, the butyl chains were omitted for clarity.

(Fig. 2) confirm the E-conformation of the double bonds on either side of the thienyl moieties. For **DBAT1,** one of the terminal phenyl rings shows a large 20° twist while the other is almost in plane with the thiophene vinyl moiety (twist angle of 4°) (Fig. 2a). Such a twist was apparently not observed in the structure of the reported 2,5-bis(4-styryl)thiophene.[18] **DBAT1** shows a layered packing with a slip-stack pattern (Fig. 2c). Within a layer, the intermolecular π–π distances range from 3.99 to 4.64 Å. For **DBAT2**, two separate structures coexist within the crystal with twist angles of the two terminal phenyl rings with respect to the bithienyl vinyl core of 10 and 16° (Fig. 2b). The bithienyl moiety for **DBAT2** is perfectly planar with no measurable twist. The compound shows a herringbone packing patten pattern with a 27° inter-plane angle (Fig. 2d).

Electronic and photoluminescence spectra

The UV-vis absorption spectra of the **DBAT*n*** series have one band in the visible (Fig. 3). The absorption maxima red-shifts from 446 nm for **DBAT1** to 489 nm for **DBAT6** (Table 1). Considering that the oligothiophene core length increases from one to six rings, the red-shift of the absorption maximum is relatively small. In a similar series, from thiophene to sexithiophene, the absorption maximum goes from 230 to 430 nm. This suggests that, in the **DBAT*n*** series, the amino groups play a major role in controlling the electronic behavior. When compared to **DH6T**, the absorption maximum for all the members of the **DBAT*n*** series is red-shifted (**DH6T** λ_{max} 432 nm), and reduced optical band gaps are observed. No solvochromism was observed when the polarity of the solvent was varied from toluene to chloroform, acetone or THF as can be expected for short, symmetrical oligomers having no dipole moment. This is unlike polymeric species, such as poly(3-hexylthiophene), which can fold over onto itself in certain solvents and thus display strong solvochromic properties due to intramolecular interactions. The band-gaps, obtained by extrapolation of the low-energy edge of the UV-vis absorption, decrease from 2.47 (**DBAT1**) to 2.19 eV (**DBAT6**). As expected, E_g decreases as the length of the thiophene bridge is expanded attaining relatively low values for the longest members of the series.

For **DH2E4T**, the UV-vis spectrum shows a maximum at 470 nm with a well-defined shoulder at 496 nm in chloroform and show an optical band gap of 2.32 eV. Again, no solvochromism was observed with this molecule. The absorbance maximum of **DH2E4T** is strongly red shifted with respect to that of **DH6T** (470 nm *vs.* 432 nm).

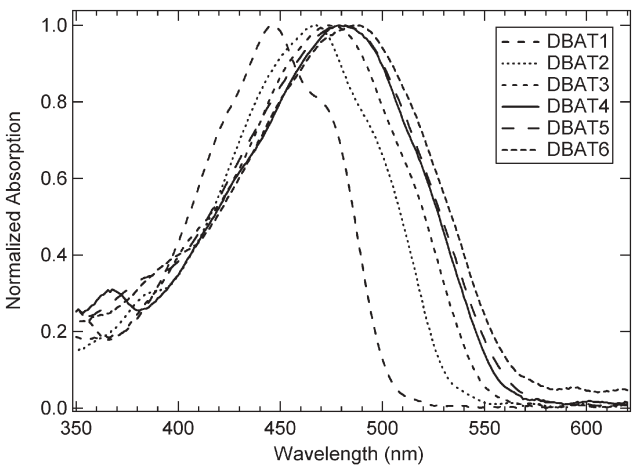

Fig. 3 UV-vis spectra for the **DBAT*n*** series in chloroform.

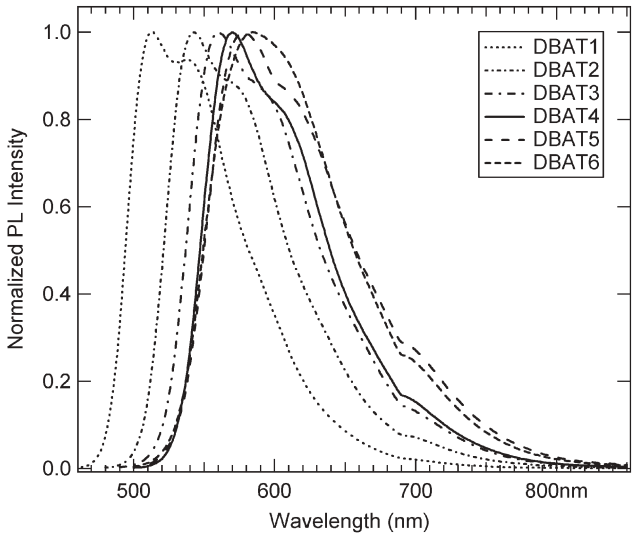

Fig. 4 Normalized photoluminescence spectra for **DBAT*n*** series in chloroform.

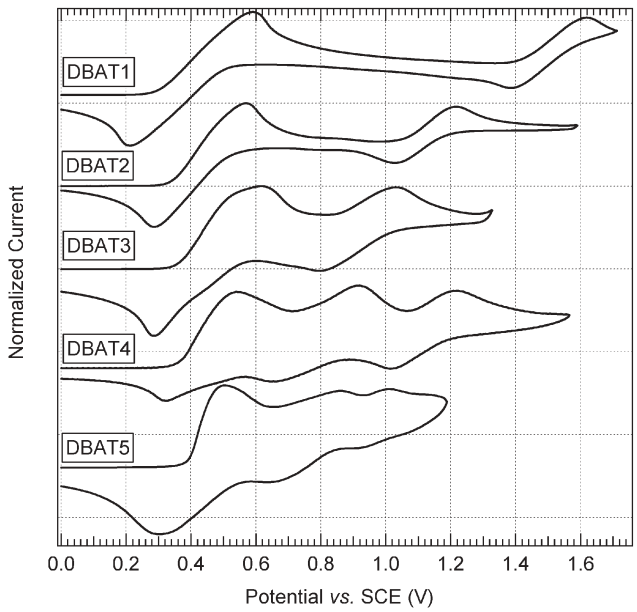

Fig. 5 Cyclic voltammograms for **DBAT1** to **-5** in CH_2Cl_2 with 0.1 M [*n*-Bu_4N][PF_6] as supporting electrolyte and at a scan rate of 100 mV s^{-1}.

All the compounds in the series show strong solution photoluminescence when excited at their absorption maximum (Fig. 4). The fluorescence maximum red-shifts with the lengthening of the bridge as expected for such conjugated structures. For several compounds within the series, no variations in their fluorescence spectrum were observed when the excitation wavelength was varied. This shows that independent from the excitation wavelength, the emission came from the same excited state.

Electrochemistry

The compounds' electrochemical behavior was investigated by cyclic voltammetry (CV) in solution and the redox potentials are summarized in Table 2. All compounds in the **DBAT*n*** series show a first oxidation wave, which is twice as large as the second oxidation wave (Fig. 5). This 2-electron oxidation was assigned to the simultaneous oxidation of the terminal amino moieties. The potential of this redox wave, close to 0.4 V *vs.* SCE, remain almost constant throughout the **DBAT*n*** series, irrespective to the extent of the conjugated system (Fig. 5). A similar behavior was reported for a series of bis(phenyl)amino-capped oligothiophenes.[19,20] It was observed that the 1st oxidation waves are very broad, which is likely due to a combination of the relatively poor electrochemical solvent (methylene chloride) combined to the simultaneous oxidation of the two amino groups. However, no splitting of this wave was seen on the voltammograms, even at slow scan rates, which indicates that little or no electronic communication is observed through the conjugated bridge between the two amino moieties even with the shortest bridge (*i.e.* **DBAT1**).

The potential of the third oxidation process however decreases from 1.40 V for **DBAT1** to 0.75 V for **DBAT5**. This potential was assigned to the first oxidation of the oligothiophene bridge. The shift to lower redox potentials with the lengthening of the bridge is consistent with increasing conjugation length from one to five thiophene rings and a similar behavior has frequently been reported in the literature.[4] It is to be noted that the DBAT compounds were sturdy and able to withstand multiple oxidations without decomposition as attested by the reversibility of the first two oxidation waves. Unfortunately, as the solubility of **DBAT6** in CH_2Cl_2 was too low, a CV could not be measured in this solvent. In THF however, **DBAT6** shows a first oxidation wave at 0.53 V *vs.* SCE. For the remaining compounds of the series, the first

Table 2 Electrochemical properties of the **DBAT*n*** series

Compound	$E_{1/2}$ oxidation/V *vs.* SCE[a]	$E_{1/2}$ reduction/V *vs.* SCE[b]	E_g^{Echem}/eV[c]	E_g^{Opt}/eV
DBAT1	0.40, 1.50	−2.27[d]	2.42	2.47
DBAT2	0.43, 1.12, 1.70[d]	−2.19, −2.30[d]	2.41	2.33
DBAT3	0.45, 0.91, 1.37, 1.63[d]	−2.00,[d] −2.18[d]	2.27	2.26
DBAT4	0.43, 0.79, 1.12	−1.83, −1.94	2.28	2.23
DBAT5	0.40, 0.75, 0.96	−1.80[d]	2.21	2.21
DBAT6	0.53[e]	−1.81, −1.91	2.19	2.19
DH2E4T	0.33, 0.88[d]	−1.96	2.29	2.32

[a] In CH_2Cl_2 with 0.1 M [NBu_4][PF_6] as supporting electrolyte, scan rate 100 mV s^{-1}. [b] In THF with 0.1 M [NBu_4][PF_6] as supporting electrolyte, scan rate 100 mV s^{-1}. [c] Measured at the onset of the first oxidation and reduction waves in THF (Fig. 5). [d] Irreversible wave. [e] CV taken in THF due to the poor solubility of **DBAT6** in CH_2Cl_2.

oxidation in THF was also constantly found close to 0.5 V (Fig. 6). Therefore, it can be concluded that in all the compounds of the series, the amino moieties oxidize first, followed by the oligothiophene bridge. At higher potential (Table 2), one to two additional oxidation waves were observed. The latter waves were irreversible which indicates the probable decomposition of the compounds.

As no reduction potentials could be observed with methylene chloride as the solvent, the reduction potentials were measured in THF. In all cases, it was possible to record the first oxidation wave within the same scan as the reduction wave, thus allowing for a direct measurement of the electrochemical band gap (E_g^{Echem}). Voltammograms in THF for a few representative compounds are shown in Fig. 6. With the exception of **DBAT1**, the compounds of the **DBAT*n*** series showed two closely spaced reductions (Table 2), whose potentials increase with increasing oligothiophene chain length. The reduction waves are not reversible up to **DBAT3**, at which point both waves become reversible.

The energy gap, which was measured at the onset of the first reduction and oxidation waves in THF, decreases throughout the series with increased oligothiophene bridge length and the values obtained from the electronic spectra and from the cyclic voltammograms are in good agreement following the same decreasing trend. It is interesting that the trend seen for E_g is mainly due to an increase in electron affinity from **DBAT1** to **DBAT6** while the first ionization potential (the oxidation of the amine capping group) shows little dependence on the length of the conjugated system.

DH2E4T shows two oxidation waves at 0.33 and 0.88 V with the second wave being irreversible. In THF, a reduction wave was recorded at −1.96 V. The band gap value for **DH2E4T** (2.29 V) is comparable to **DBAT2** or **-3** although its ionization potential is slightly greater. Both the 1st oxidation process and band gap value for **DH2E4T** are comparable with other EDOT-thiophene-based oligomers of comparable lengths recently published in the literature.[21–24]

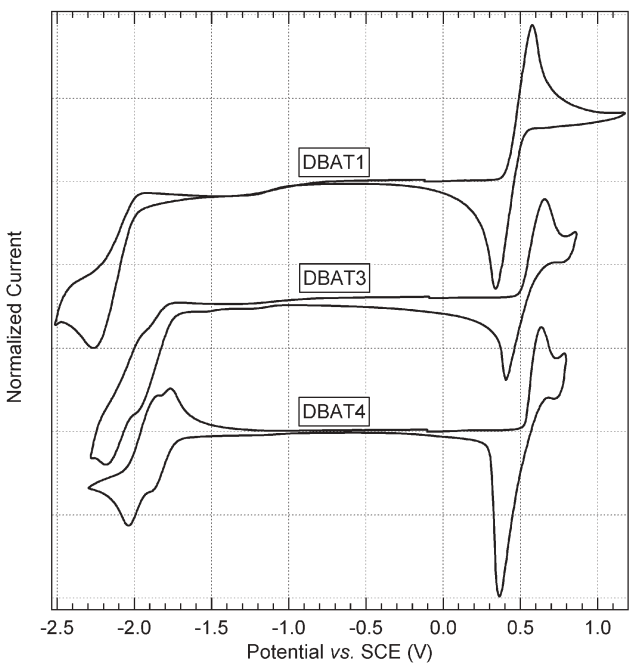

Fig. 6 Cyclic voltammograms for **DBAT1**, **DBAT3** and **BDAT4** in THF with 0.1 M [*n*-Bu_4N][PF_6] as supporting electrolyte and at a scan rate of 100 mV s^{-1}.

Conclusion

In conclusion, we have prepared a series of novel conjugated thiophene-based oligomers that exhibit good thermal stability as well as interesting electronic and solid-state properties. Throughout the **DBAT*n*** series, we found that the energy gap and electron affinity are dependent on the length of the conjugated bridge while the ionization potential remains almost constant, being dominated by the amino capping groups. We also showed clearly the crystal packing dependence on the odd or even number of thiophene units contained in the bridge. This is apparent in the visual aspect of spin-coated films, the unusual variations in melting points and preliminary X-ray crystal structure determinations. Further solid-state studies to elucidate this behavior including thin film XRD and single crystal studies are being pursued. **DH2E4T** was found to compare favorably with **DH6T** with respect to energy gap, ionization potential and electron affinity, but with greater solubility. Charge carrier mobility measurements and use of all the compounds as the hole transport layer in solar energy conversion are in progress.

Experimental section

2,5-Thiophene dicarboxaldehyde,[25] 5,5′-(2,2′-bithiophene) dicarboxaldehyde,[25] 5,5″-(2,2′:5′,2″-terthiophene) dicarboxaldehyde,[14] 5,5′-dibromo-2,2′-bithiophene,[11] 5-bromo-5′-formyl-2,2′-bithiophene,[14] 2,5-bis(tributylstannyl)thiophene,[14] 5,5′-bis(tributylstannyl)-2,2′-bithiophene,[14] and 5,5′-bis(tributylstannyl)-2,2′-bis(3,4-ethylenedioxythiophene)[26] were prepared following literature procedures. Diethyl-[4-(*N*,*N*-dibutyl)aminobenzyl] phosphonate was prepared by refluxing commercially available diethyl-(4-aminobenzyl) phosphonate (Aldrich) with K_2CO_3 in ten equivalents of bromobutane as the solvent. THF and diethyl ether were dried over sodium–benzophenone and distilled fresh before use. All other reagents were purchased from Sigma-Aldrich or Fisher Chemicals and used as received without further purification. ^{1}H NMR spectra were taken on a Varian Unity INOVA AS400 spectrometer at 400 MHz and referenced to residual solvent. Elemental analyses were performed at Huffman Laboratories (Golden, CO). DSC analyses were done on a TA Instruments DSC 2910 at 10 °C min^{-1}. TGA analyses were done on a TA Instruments TGA2950 at 5 °C min^{-1}. UV-vis spectra were taken on a Varian Cary 500 spectrophotometer. Emission spectra were taken on a Fluorolog 1680 spectrophotometer. Cyclic voltammetry was done on a Pine AFCBP1 bipotentiostat with a platinum disk working electrode, a platinum coil counter electrode and a silver wire quasi reference electrode. Decamethylferrocene (Strem) was added to the electrolyte solution as an internal reference and the potentials corrected *vs.* SCE.[27]

General procedure for DBAT1, DBAT2 and DBAT3

To a stirred THF solution of diethyl-[4-(*N*,*N*-dibutyl)aminobenzyl] phosphonate and the appropriate thiophene dicarboxaldehyde (cooled at 5 °C under argon) was very slowly added a solution of potassium *tert*-butoxide in THF. After the addition, the mixture was stirred for 1 h at 25 °C. The reaction mixture was poured in sat. $NaHCO_3$, and the aqueous layer extracted with diethyl ether. The combined organic fractions were washed with water and dried over $MgSO_4$. Removal of the solvent yielded the crude product which was purified by recrystallization from a hot methylene chloride–methanol mixture.

2,5-Bis[(*E*,*E*)-(4-*N*,*N*-dibutylaminobenzylidene)methyl]thiophene (DBAT1). The general procedure was followed with 2,5-thiophene dicarboxaldehyde (0.70 g, 5.00 mmol), diethyl-[4-(*N*,*N*-dibutyl)aminobenzyl]phosphonate (3.91 g, 11.0 mmol) in 30 mL of THF and *t*-BuOK (11.5 mL, 1 M in THF diluted with 30 mL of THF, 11.5 mmol). The product (2.17 g, 80%) was obtained as an orange powder (Found: C 79.84; H 9.11; N 5.15. $C_{36}H_{50}N_2S$ requires C, 79.70; H, 9.23; N, 5.17%); δ_H (400 MHz; $CDCl_3$; Me_4Si) 7.30 (2 H, d, *J* 8.2, NPh), 6.94 (1 H, d, *J* 16.0, Ph–CH_2=CH$_2$–), 6.72–6.82 (2 H, m Ph–CH$_2$=CH_2– and Th-*H*), 6.60 (2, H, d, *J* 8.2, NPh), 3.28 (4 H, t, *J* 7.6, 2 × NCH_2CH$_2$CH$_2$CH$_3$), 1.57 (4 H, m, 2 × NCH$_2$CH_2CH$_2$CH$_3$), 1.35 (4 H, m, 2 × NCH$_2$CH_2CH$_2$CH$_3$), 0.95 (6 H, t, *J* 7.2, 2 × NCH$_2$CH$_2$CH$_2$CH_3).

5,5′-Bis[(*E*,*E*)-(4-*N*,*N*-dibutylaminobenzylidene)methyl]-2,2′-bithiophene (DBAT2). The general procedure was followed with 5,5′-bithiophene dicarboxaldehyde (1.25 g, 5.62 mmol), diethyl-[4-(*N*,*N*-dibutyl)aminobenzyl] phosphonate (4.22 g, 11.9 mmol) in 100 mL of THF and ^{t}BuOK (12.4 mL, 1 M in THF, diluted with 30 mL of THF, 12.4 mmol). The product (2.59 g, 74%) was obtained as a red powder (Found: C 76.53; H 8.22; N 4.48. $C_{40}H_{52}N_2S_2$ requires C, 76.92; H, 8.33; N, 4.49%); δ_H (400 MHz; $CDCl_3$; Me_4Si) 7.30 (2 H, d, *J* 8.2, NPh), 7.00 (1 H, d, *J* 3.8, Th-H4), 6.93 (1 H, d, *J* 16.0, Ph–CH_2=CH$_2$–), 6.83 (1 H, d, *J* 3.8, Th-H3), 6.79 (1 H, m Ph–CH$_2$=CH_2–), 6.59 (2 H, d, *J* 8.2, NPh), 3.27 (4 H, t, *J* 7.6, 2 × NCH_2CH$_2$CH$_2$CH$_3$), 1.56 (4 H, m, 2 × NCH$_2$CH_2CH$_2$CH$_3$), 1.35 (4 H, m, 2 × NCH$_2$CH_2CH$_2$CH$_3$) and 0.95 (6 H, t, *J* 7.2, 2 × NCH$_2$CH$_2$CH$_2$CH_3).

5,5″-Bis[(*E*,*E*)-(4-*N*,*N*-dibutylaminobenzylidene)methyl]-2,2′:5′,2″-terthiophene (DBAT3). The general procedure was followed with 5,5″-terthiophene dicarboxaldehyde (0.72 g, 2.37 mmol), diethyl-[4-(*N*,*N*-dibutyl)aminobenzyl] phosphonate (1.85 g, 5.21 mmol) in 90 mL of THF and ^{t}BuOK (5.50 mL, 1 M in THF, diluted with 10 mL of THF, 5.50 mmol). The product (1.27 g, 76%) was obtained as a red powder (Found: C 74.49; H 7.73; N 4.00. $C_{44}H_{54}N_2S_3$ requires C, 74.79; H, 7.65; N, 3.97%); δ_H (400 MHz; $CDCl_3$; Me_4Si) 7.30 (d, 2 H, d, *J* 8.2, NPh), 7.00–7.05 (2 H, m, Th-H4 and Th-H3′), 6.93 (1 H, d, *J* 16.0, Ph–CH_2=CH$_2$–), 6.83 (1 H, d, *J* 3.8, Th-H3), 6.78 (1 H, d, *J* 16.0, Ph–CH$_2$=CH_2–), 6.59 (2 H, d, *J* 8.2, NPh), 3.27 (4 H, t, *J* 7.6, 2 × NCH_2CH$_2$CH$_2$CH$_3$), 1.56 (4 H, m, 2 × NCH$_2$CH_2CH$_2$CH$_3$), 1.35 (4 H, m, 2 × NCH$_2$CH_2CH$_2$CH$_3$), 0.95 (6 H, t, *J* 7.2, 2 × NCH$_2$CH$_2$CH$_2$CH_3).

2-[(*E*)-(4-*N*,*N*-Dibutylaminobenzylidene)methyl]thiophene (1). This molecule is a slight variation from a known compound.[28] The general procedure for **DBAT1** was followed with 2-thiophene carboxaldehyde (1.49 g, 13.3 mmol), diethyl-[4-(*N*,*N*-dibutyl)aminobenzyl] phosphonate (4.30 g, 12.1 mmol) in 30 mL of THF and ^{t}BuOK (13.5 mL, 1 M in THF, diluted with 15 mL of THF, 13.5 mmol). The crude product was purified with a silica gel plug eluted with hexanes–ethyl acetate (9 : 1 *v*/*v*). The first yellow band was collected and the product obtained as a yellow oil (3.82 g, 91%). δ_H (400 MHz; $CDCl_3$; Me_4Si) 7.30 (d, 2 H, d, *J* 8.8, NPh), 7.08 (1 H, m, Th-H), 6.98 (1 H, d, *J* 16.0, Ph–CH_2=CH$_2$–), 6.95 (2 H, m, 2 × Th-H), 6.83 (1 H, d, *J* 16.0, Ph–CH$_2$=CH_2–), 6.59 (d, 2 H, d, *J* 8.8, NPh), 3.26 (4 H, t, *J* 7.6, 2 × NCH_2CH$_2$CH$_2$CH$_3$), 1.56 (4 H, m, 2 × NCH$_2$CH_2CH$_2$CH$_3$), 1.34 (4 H, m, 2 × NCH$_2$CH_2CH$_2$CH$_3$) and 0.94 (6 H, t, *J* 7.2, 2 × NCH$_2$CH$_2$CH$_2$CH_3).

(2-Tributylstannyl-5-[(*E*)-(4-*N*,*N*-dibutylaminobenzylidene)-methyl]thiophene (2). To a solution of 2-[4-(*N*,*N*-dibutyl-amino)styryl]-thiophene (3.10 g, 9.90 mmol) in THF (90 mL) at −78 °C was added dropwise *n*-BuLi (4.50 mL, 2.5 M solution in hexanes, 11.0 mmol). After the addition, the mixture was stirred for 1 h at −78 °C and then the temperature was raised to 25 °C. Tributylstannyl chloride (4.22 g, 13.0 mmol) was added slowly and the reaction stirred for 1 h. The mixture was diluted with hexanes (250 mL) and washed with sat. $NaHCO_3$, water and dried over $MgSO_4$. Removal of the solvent yielded a brown oil which was used without further purification. δ_H (400 MHz; $CDCl_3$; Me_4Si) 7.30 (d, 2 H, d, *J* 8.8, NPh), 7.06 (1 H, d, *J* 3.2, Th-H4), 7.03 (1 H, d, *J* 16.0, Ph–CH_2=CH$_2$–), 7.02 (1 H, d, *J* 3.2, Th-H3), 6.84 (1 H, d, *J* 16.0, Ph–CH$_2$=CH_2–), 6.58 (d, 2 H, d, *J* 8.8, NPh), 3.26 (4 H, m, 2 × NCH_2(CH$_2$)$_2$CH$_3$), 1.54 (10 H, 2 × NCH$_2$CH_2CH$_2$CH$_3$ and 3 × SnCH_2(CH$_2$)$_2$CH$_3$), 1.33 (16 H, m, 2 × N(CH$_2$)$_2$CH_2CH$_3$ and 3 × SnCH$_2$(CH_2)$_2$CH$_3$), 0.94 (15 H, m, 2 × N(CH$_2$)$_3$CH_3 and 3 × Sn(CH$_2$)$_3$CH_3).

5′-Bromo-5-[(*E*)-(4-*N*,*N*-dibutylaminobenzylidene)methyl]-2,2′-bithiophene (3). This molecule is a slight variation from a known compound.[28] The general procedure for **DBAT1** was followed with 5-bromo-5′-formyl-2,2′-bithiophene (6.91 g, 25.3 mmol), diethyl-[4-(*N*,*N*-dibutyl)aminobenzyl] phosphonate (9.89 g, 27.9 mmol) in 60 mL of THF and ^{t}BuOK (28.0 mL, 1 M in THF, diluted with 30 mL of THF, 28.0 mmol). The crude product was purified with a silica gel plug eluted with hexanes–ethyl acetate (9 : 1 *v*/*v*. The first yellow band was collected and the product obtained as an orange powder (9.82 g, 82%). δ_H (400 MHz; $CDCl_3$; Me_4Si) 7.30 d, 2 H, d, *J* 8.6, NPh), 6.95 (1 H, d, *J* 4.0, Th-H4′), 6.93 (1 H, d, *J* 4.0, Th-H3′), 6.91 (1 H, d, *J* 16.0, Ph–CH_2=CH$_2$–), 6.87 (1 H, d, *J* 4.0, Th-H4), 6.82 (1 H, d, *J* 4.0, Th-H3), 6.80 (1 H, d, *J* 16.0, Ph–CH$_2$=CH_2–), 6.59 (d, 2 H, d, *J* 8.6, NPh), 3.27 (4 H, t, *J* 7.6, 2 × NCH_2CH$_2$CH$_2$CH$_3$), 1.56 (4 H, m, 2 × NCH$_2$CH_2CH$_2$CH$_3$), 1.34 (4 H, m, 2 × NCH$_2$CH_2CH$_2$CH$_3$) nad 0.95 (6 H, t, *J* 7.2, 2 × NCH$_2$CH$_2$CH$_2$CH_3).

General procedure for DBAT4, DBAT5, DBAT6 and DH2E4T

The appropriate stannylthiophene and bromothienyl starting materials were dissolved in DMF, argon was bubbled through the solution for 30 min and $Pd(PPh_3)_4$ was then added. The reaction mixture was heated to 100 °C for 18 h under argon. After cooling, the mixture was poured into 300 mL of methanol under vigorous stirring. The resulting red suspension was stirred for 30 min and the suspended solid filtered. The crude material was recrystallized from neat acetone or methylene chloride–methanol.

5,5‴-Bis[(*E*,*E*)-(4-*N*,*N*-dibutylaminobenzylidene)methyl]-2,2′:5′,2″:5″,2‴-quaterthiophene (DBAT4). The general procedure was followed with **2** (6.00 g, 9.97 mmol), 5,5′-dibromo-2,2′-bithiophene (1.29 g, 3.99 mmol) and $Pd(PPh_3)_4$ (0.15 g, 0.13 mmol) in DMF (60 mL). **DBAT4** (2.16 g, 69%) was obtained as a bright red powder from acetone (Found: C 73.31; H 7.10; N 3.43. $C_{48}H_{56}N_2S_4$ requires C, 73.10; H, 7.11; N, 3.55%); δ_H (400 MHz; $CDCl_3$; Me_4Si) 7.31 (2 H, d, *J* 8.8, NPh), 7.01–7.07 (3 H, m, 3 × Th-H), 6.93 (1 H, d, *J* 16.0, Ph–C*H*$_2$=CH$_2$–), 6.85 (1 H, d, *J* 3.8, Th-H3), 6.81 (1 H, d, *J* 16.0, Ph–CH$_2$=C*H*$_2$–), 6.57 (2 H, d, *J* 8.8, NPh), 3.28 (4 H, t, *J* 7.6, 2 × NC*H*$_2$CH$_2$CH$_2$CH$_3$), 1.56 (4 H, m, 2 × NCH$_2$C*H*$_2$CH$_2$CH$_3$), 1.35 (4 H, m, 2 × NCH$_2$C*H*$_2$CH$_2$CH$_3$), 0.95 (6 H, t, *J* 7.2, 2 × NCH$_2$CH$_2$CH$_2$C*H*$_3$).

5,5‴′-Bis[(*E*,*E*)-(4-*N*,*N*-dibutylaminobenzylidene)methyl]-2,2′:5′,2″:5″,2‴:5‴,2‴′-quinquethiophene (DBAT5). The general procedure was followed with **3** (4.00 g, 8.44 mmol), 2,5-bis(tributylstannyl)thiophene (2.54 g, 3.84 mmol) and $Pd(PPh_3)_4$ (0.10 g, 0.09 mmol) in DMF (60 mL). The crude material was recrystallized from methylene chloride–methanol to yield **DBAT5** (1.73 g, 52%) as a red powder (Found: C 71.80; H 6.51; N 2.99. $C_{50}H_{58}N_2S_5$ requires C, 71.72; H, 6.67; N, 3.22%); δ_H (400 MHz; $CDCl_3$; Me_4Si) 7.31 (2 H, d, *J* 9.2, NPh), 7.02–7.08 (4 H, m, 4 × Th-H), 6.93 (1 H, d, *J* 16.0, Ph–C*H*$_2$=CH$_2$), 6.85 (1 H, d, *J* 4.0, Th-H3), 6.81 (1 H, d, *J* 16.0, Ph–CH$_2$=C*H*$_2$), 6.59 (2 H, d, *J* 9.2, NPh), 3.27 (4 H, t, *J* 7.6, 2 × NC*H*$_2$CH$_2$CH$_2$CH$_3$), 1.56 (4 H, m, 2 × NCH$_2$C*H*$_2$CH$_2$CH$_3$), 1.35 (4 H, m, 2 × NCH$_2$C*H*$_2$CH$_2$CH$_3$) and 0.95 (6 H, t, *J* 7.2, 2 × NCH$_2$CH$_2$CH$_2$C*H*$_3$).

5,5⁗-Bis[(*E*,*E*)-(4-*N*,*N*-dibutylaminobenzylidene)methyl]-2,2′:5′,2″:5″,2‴:5‴,2‴′:5⁗,2⁗-sexithiophene (DBAT6). The general procedure was followed with **3** (2.80 g, 5.91 mmol), 5,5′-bis(tributylstannyl)-2,2′-bithiophene (2.00 g, 2.69 mmol) and $Pd(PPh_3)_4$ (70.0 mg, 0.06 mmol) in DMF (50 mL). The crude material was recrystallized from methylene chloride–methanol to give **DBAT6** (0.73 g, 35%) as a fine dark red powder (Found: C 70.49; H 6.38; N 3.04. $C_{52}H_{60}N_2S_6$ requires C, 70.59; H, 6.30; N, 2.94%); δ_H (400 MHz; $CDCl_3$; Me_4Si) 7.31 (2 H, d, *J* 8.8, NPh), 7.02–7.08 (5 H, m, 5 × Th-H), 7.93 (1 H, d, *J* 16.0, Ph–C*H*$_2$=CH$_2$), 6.85 (1 H, d, *J* 4.0, Th-H3), 6.80 (1 H, d, *J* 16.0, Ph–CH$_2$=C*H*$_2$), 6.59 (2 H, d, *J* 8.8, NPh), 3.27 (4 H, t, *J* 7.6, 2 × NC*H*$_2$CH$_2$CH$_2$CH$_3$), 1.56 (4 H, m, 2 × NCH$_2$C*H*$_2$CH$_2$CH$_3$), 1.35 (4 H, m, 2 × NCH$_2$CH$_2$C*H*$_2$CH$_3$) and 0.95 (6 H, t, *J* 7.2, 2 × NCH$_2$CH$_2$CH$_2$C*H*$_3$)

5,5′-Bis[(2-hexyl-2,2′-bithien-5′-yl)]-2,2′-bis(3,4-ethylenedioxythiophene) (DH2E4T). The general procedure was followed with 5-bromo-5′-hexyl-2,2′-bithiophene (2.71 g, 8.25 mmol), 5,5′-bis(tributylstannyl)-2,2′-bis(3,4-ethylenedioxythiophene) (2.80 g, 3.30 mmol) and $Pd(PPh_3)_4$ (50.0 mg, 0.04 mmol) in DMF (60 mL). The crude product was recrystallized from acetone to give **DH2E4T** (1.08 g, 42%) as an orange crystalline powder (Found: C 61.35; H 5.48. $C_{40}H_{42}O_4S_6$ requires C, 61.70; H, 5.40%); δ_H (400 MHz; THF-d_8; Me_4Si) 7.10 (1 H, d, *J* 4.0, Th-H4′), 7.03 (1 H, d, *J* 4.0, Th-H3′), 6.99 (1 H, d, *J* 4.0, Th-H4), 6.70 (1 H, dt, *J* 4.0 and 0.8, Th-H3), 4.41 (4 H, s, –OC*H*$_2$C*H*$_2$O–), 2.80 (2 H, t, *J* 7.4, Th–C*H*$_2$(CH$_2$)$_4$CH$_3$), 1.69 (2 H, t, *J* 7.4, Th–CH$_2$C*H*$_2$(CH$_2$)$_3$CH$_3$), 1.43–1.34 (6 H, m, Th–(CH$_2$)$_2$(C*H*$_2$)$_3$CH$_3$) and 0.91 (3 H, m, Th–(CH$_2$)$_5$C*H*$_3$).

X-Ray crystallography of DBAT1 and -2‡. Crystals suitable for X-ray diffraction studies were grown from chloroform–methanol solutions at room temperature. A crystal of **DBAT1** (orange) or **-2** (red) of appropriate size was mounted on a glass fiber using Paratone-N oil, transferred to a Siemens SMART diffractometer/CCD area detector, centered in the beam (Mo Kα; λ = 0.71073 Å; graphite monochromator), and cooled to −116 °C by a nitrogen low-temperature apparatus (which had been previously calibrated by thermocouple) placed at the same position as the crystal. Preliminary orientation matrix and cell constants were determined by collection of 60 10-s frames, followed by spot integration and least-squares refinement. A minimum of a hemisphere of data was collected using 0.3° *?* scans at 30 s per frame. The raw data were integrated and the unit cell parameters refined using SAINT. Data analysis was performed using XPREP. Absorption correction was applied using SADABS. The data were corrected for Lorentz and polarization effects, but no correction for crystal decay was applied. Structure solutions and refinements were performed (SHELXTL-Plus V5.0) on F-squared. Refer to the electronic supplementary information for more data.

DBAT1: Preliminary data indicated a monoclinic cell. The choice of the centric space group $P2_1/n$ (#14) was confirmed by the successful solution and refinement of the structure. Disorder on two of the alkyl chains was modelled. The occupancy of all the disordered atoms was refined isotropically. The same *x*, *y*, and *z* parameters and isotropic displacement parameters were used for the following pairs of atoms: C15, C15A; C35, C35A. This was done using the EXYZ and EADP line commands. Constraints were placed on bond distances within one of the alkyl chains in order to achieve uniformity. The extinction coefficient refined to 0.0023. All other non-H atoms were refined anisotropically. All H-atoms were placed in idealized positions and were included in structure factor calculations but were not refined. Crystal data for **DBAT1**: $C_{36}H_{50}N_2S$, *M* = 542.84, monoclinic, space group $P2_1/n$ (#14), *a* = 12.301(5) Å, *b* = 16.426(6) Å, *c* = 16.316(7) Å, α = 90°, β = 99.026(9)°, γ = 90°, *U* = 3256(2) Å^3, *Z* = 4, *T* = −116 °C, μ(Mo Kα) = 1.9 mm^{-1}, 18719 reflections measured from which 4536 (R_{int} 0.0974) were independent, wR_2 (all data) = 0.2232.

DBAT2: Preliminary data indicated a triclinic cell. The choice of the centric space group P-1 (#2) was confirmed by

the successful solution and refinement of the structure. Disorder on two of the alkyl chains was modelled. The occupancy of all the disordered atoms was refined isotropically. The same x, y, and z parameters and isotropic displacement parameters were used for the following pairs of atoms: C33, C33A; C39, C39A. This was done using the EXYZ and EADP line commands. All other non-H atoms were refined anisotropically. All H-atoms were placed in idealized positions and were included in structure factor calculations but were not refined. Crystal data for **DBAT2**: $C_{40}H_{52}N_2S_2$, M = 624.96, triclinic, space group P-1 (#2), a = 12.0888(6) Å, b = 12.1517(7) Å, c = 12.8142 Å, α = 84.4140(10)°, β = 73.1610(10)°, γ = 87.552(2)°, U = 1792.92(16) Å^3, Z = 2, T = −116 °C, μ(Mo Kα) = 1.9 mm^{-1}, 14383 reflections measured from which 3229 (R_{int} 0.0659) were independent, wR_2 (all data) = 0.2708.

Acknowledgements

This research was supported by Xcel Energy, contract FIA-021521. We thank Dr Joe Bozell for the gracious loan of his synthetic laboratory space.

References

1 S. E. Shaheen, D. S. Ginley and G. E. Jabbour, *MRS Bull.*, 2005, **30**, 10–19.
2 B. O'Reagan and M. Gratzel, *Nature*, 1991, **353**, 737–740.
3 S. E. Shaheen and D. S. Ginley, in *Dekker Encyclopedia of Nanoscience of Nanotechnology*, ed. J. A. Schwarz, C.I. Contescu and K. Putyera, Marcel Dekker, Inc., New York, 2004, pp. 2879–2895.
4 K. Müllen and G. Wegner, *Electronic Materials: The Oligomer Approach*, Wiley-VCH, Weinheim, 1998.
5 U. Mitschke and P. Bäuerle, *J. Mater. Chem.*, 2000, **10**, 1471–1507.
6 M. Grätzel, *Nature*, 2003, **421**, 586–587.
7 F. Garnier, A. Yassar, R. Hajlaoui, G. Horowitz, F. Deloffre, B. Servet, S. Ries and P. Alnot, *J. Am. Chem. Soc.*, 1993, **115**, 8716–8721.
8 F. Garnier, *Acc. Chem. Res.*, 1999, **32**, 209–215.
9 P. Bäuerle, in *Electronic Materials: The Oligomeric Approach*, ed. K. Müllen, G. Wegner,Wiley-VCh, Weinheim, 1998, pp. 105–197.
10 P. Bäuerle, In *Handbook of Oligo- and Polythiophenes*, ed. D. Fichou, Wiley-VCH, Weinheim, 1998, pp. 89–184.
11 C. Van Pham, A. Burkhardt, R. Shabana, D. D. Cunningham, H. B. J. Mark and H. Zimmers, *Phosphorus, Sulfur Silicon Relat. Elem.*, 1989, **46**, 153–168.
12 P. Frère, J. M. Raimundo, P. Blanchard, J. Delaunay, P. Richomme, J. L. Sauvajol, J. Orduna, J. Garin and J. Roncali, *J. Org. Chem.*, 2003, **68**, 7254–7265.
13 G. Götz, S. Scheib, R. Klose, J. Heinze and P. Bäuerle, *Adv. Funct. Mater.*, 2002, **12**, 723–728.
14 Y. Wei, Y. Yang and J.-M. Yeh, *Chem. Mater.*, 1996, **8**, 2659–2666.
15 G. Barbarella, D. Casarini, M. Zambianchi, L. Favaretto and S. Rossini, *Adv. Mater.*, 1996, **8**, 69–73.
16 R. Azumi, M. Goto, K. Honda and M. Matsumoto, *Bull. Chem. Soc. Jpn.*, 2003, **76**, 1561–1567.
17 M. Melucci, M. Gazzano, G. Barbarella, M. Cavallini, F. Biscarini, P. Maccagnani and P. Ostoja, *J. Am. Chem. Soc.*, 2003, **125**, 10266–10274.
18 V. D. Zobel and G. Ruban, *Acta Crystallogr., Sect. B: Struct. Crystallogr. Cryst. Chem.*, 1978, **34**, 1652–1657.
19 T. Noda, I. Imae, N. Noma and Y. Shirota, *Adv. Mater.*, 1997, **9**, 239–241.
20 T. Noda, H. Ogawa, N. Noma and Y. Shirota, *Adv. Mater.*, 1997, **9**, 720–722.
21 M. Turbiez, P. Frère, M. Allain, C. Videlot, J. Ackermann and J. Roncali, *Chem.–Eur. J.*, 2005, **11**, 3742–3752.
22 M. Turbiez, P. Frère and J. Roncali, *J. Org. Chem.*, 2003, **68**, 5357–5360.
23 J. J. Apperloo, L. Groenendaal, H. Verheyen, M. Jayakannan, R. A. J. Janssen, A. Dkhissi, D. Beljonne, R. Lazzaroni and J. L. Brédas, *Chem.–Eur. J.*, 2002, **8**, 2384–2396.
24 R. G. Hicks and M. B. Nodwell, *J. Am. Chem. Soc.*, 2000, **122**, 6746–6753.
25 Y. Wei, B. Wang, W. Wang and J. Tian, *Tetrahedron Lett.*, 1995, **36**, 665–668.
26 A. K. Mohanakishnan, A. Hucke, M. A. Lyon, M. V. Lakshmikantham and M. P. Cava, *Tetrahedron*, 1999, **55**, 11745–11754.
27 A. J. Bard and L. R. Faulkner, *Electrochemical Methods, Fundamentals and Applications*, John Wiley & Sons, New York, 1980.
28 J.-M. Raimundo, P. Blanchard, N. Gallego-Planas, N. Mercier, I. Ledoux-Rak, R. Hierle and J. Roncali, *J. Org. Chem.*, 2002, **67**, 205–218.

